Supporting Information

Determination of Relative Tensor Orientations by γ-encoded Chemical Shift Anisotropy/Heteronuclear Dipolar Coupling 3D NMR Spectroscopy in Biological Solids

Guangjin Hou,[a,b] Sivakumar Paramasivam,[a] In-Ja L. Byeon,[b,c] Angela M. Gronenborn,[b,c] Tatyana Polenova*[a,b]

[a]*Department of Chemistry and Biochemistry, University of Delaware, Newark, Delaware 19716, United States;*

[b]*Pittsburgh Center for HIV Protein Interactions, University of Pittsburgh School of Medicine, 1051 Biomedical Science Tower 3, 3501 Fifth Ave., Pittsburgh, PA 15261, United States;*

[c]*Department of Structural Biology, University of Pittsburgh School of Medicine, 1051 Biomedical Science Tower 3, 3501 Fifth Ave., Pittsburgh, PA 15261, United States*

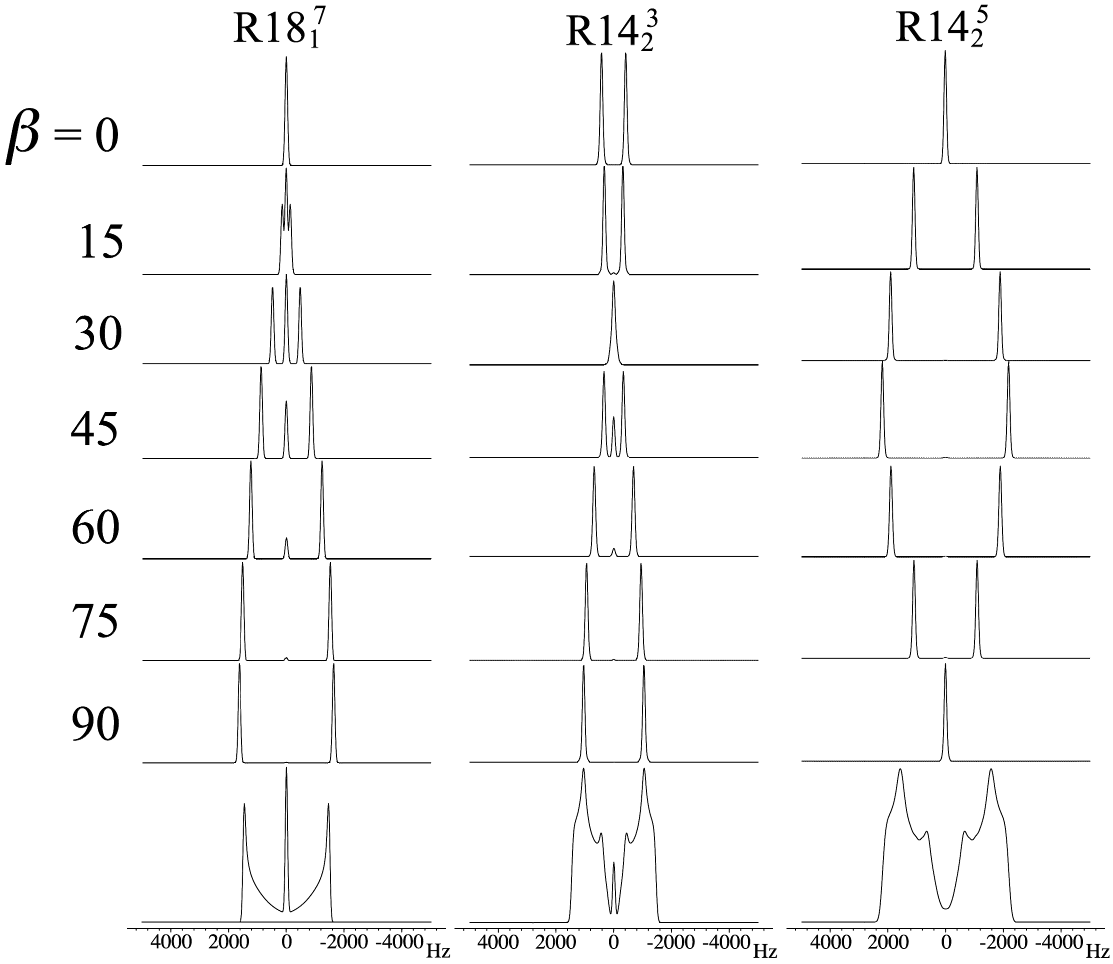

Figure S1. The recoupled ^{1}H-^{15}N dipolar and ^{15}N CSA lineshapes for different crystallite orientations in the laboratory frame produced by γ-encoded $R18_1^7$ and $R14_2^{3/5}$. Two-spin system (^{1}H, ^{15}N) is used in all simulations. The recoupled powder patterns are illstrated in the bottom figure; the powder averaged were generated using 986 ZCW crystallite orientations (α, β). As shown in the Figure, there is only one splitting corresponding to each crystallite and it is independent of the number of gamma angles. This demonstrates that $R18_1^7$ and $R14_2^{3/5}$ recoupling techniques are *γ*-encoded.

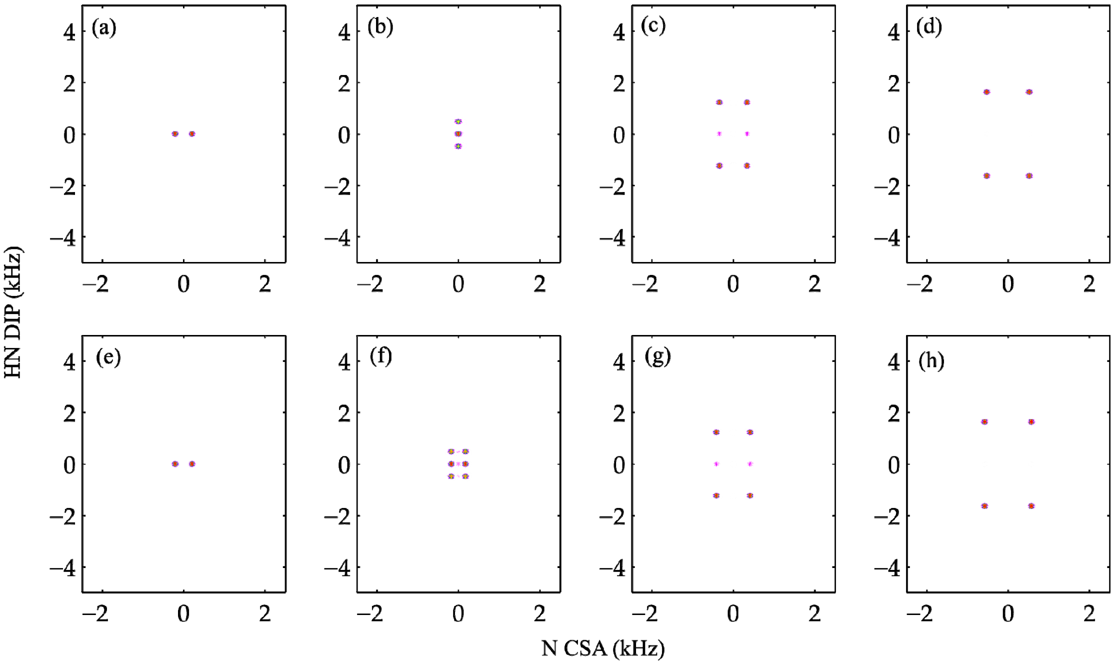

Figure S2. The simulated ^{1}H-^{15}N dipolar and ^{15}N CSA correlation spectra by the combined $R18_1^7/R14_2^3$ symmetry scheme for different crystallite orientations. The same DIP/CSA relative orientation was used for all simulations. The crystallite orientations expressed in terms of the Euler angles are (a) $\alpha = 0^o$, $\beta = 0^o$; (b) $\alpha = 0^o$, $\beta = 30^o$; (c) $\alpha = 0^o$, $\beta = 60^o$; (d) $\alpha = 0^o$, $\beta = 90^o$; (e) $\alpha = 30^o$, $\beta = 0^o$; (f) $\alpha = 30^o$, $\beta = 30^o$; (g) $\alpha = 30^o$, $\beta = 60^o$; (h) $\alpha = 30^o$, $\beta = 90^o$. It can be seen that the combined R-type symmetry scheme shows high sensitivity to the molecular orientation. Only one splitting can be found along DIP and CSA dimension for each crystallite orientation.

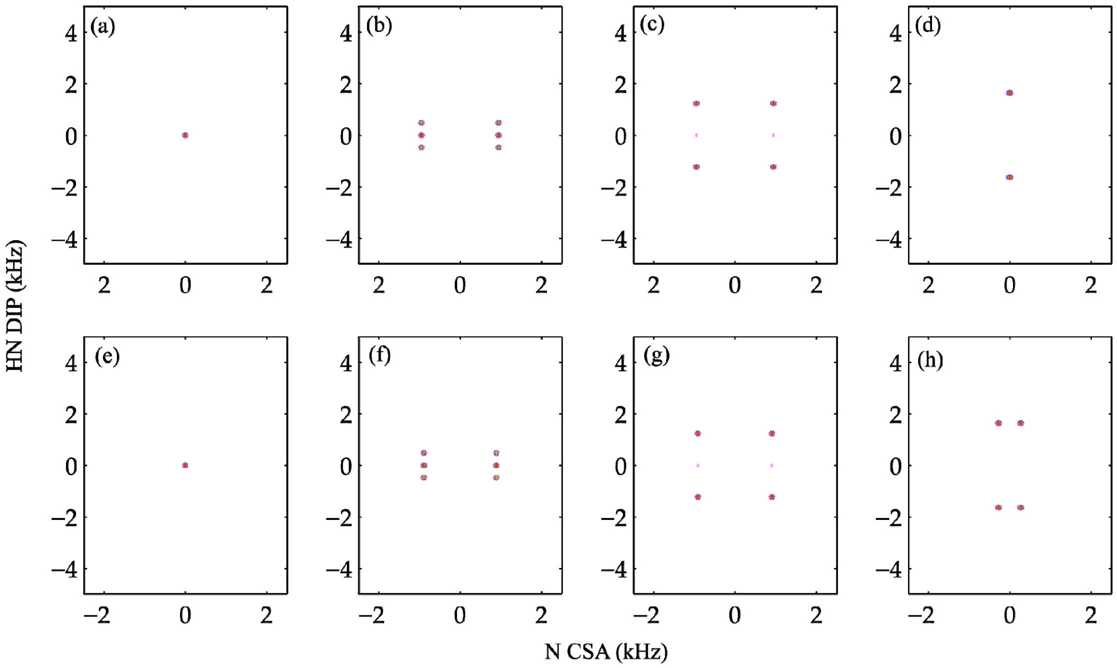

Figure S3. The simulated ^{1}H-^{15}N dipolar and ^{15}N CSA correlation spectra by the combined $R18_1^7/R14_2^5$ symmetry scheme for different crystallite orientations. The same DIP/CSA relative orientation was used for all simulations. The crystallite orientations expressed in terms of the Euler angles are (a) $\alpha = 0^o$, $\beta = 0^o$; (b) $\alpha = 0^o$, $\beta = 30^o$; (c) $\alpha = 0^o$, $\beta = 60^o$; (d) $\alpha = 0^o$, $\beta = 90^o$; (e) $\alpha = 30^o$, $\beta = 0^o$; (f) $\alpha = 30^o$, $\beta = 30^o$; (g) $\alpha = 30^o$, $\beta = 60^o$; (h) $\alpha = 30^o$, $\beta = 90^o$. As with the $R18_1^7/R14_2^3$ symmetry scheme in Figure S2, the combined $R18_1^7/R14_2^5$ symmetry scheme also shows high sensitivity to the molecular orientation.

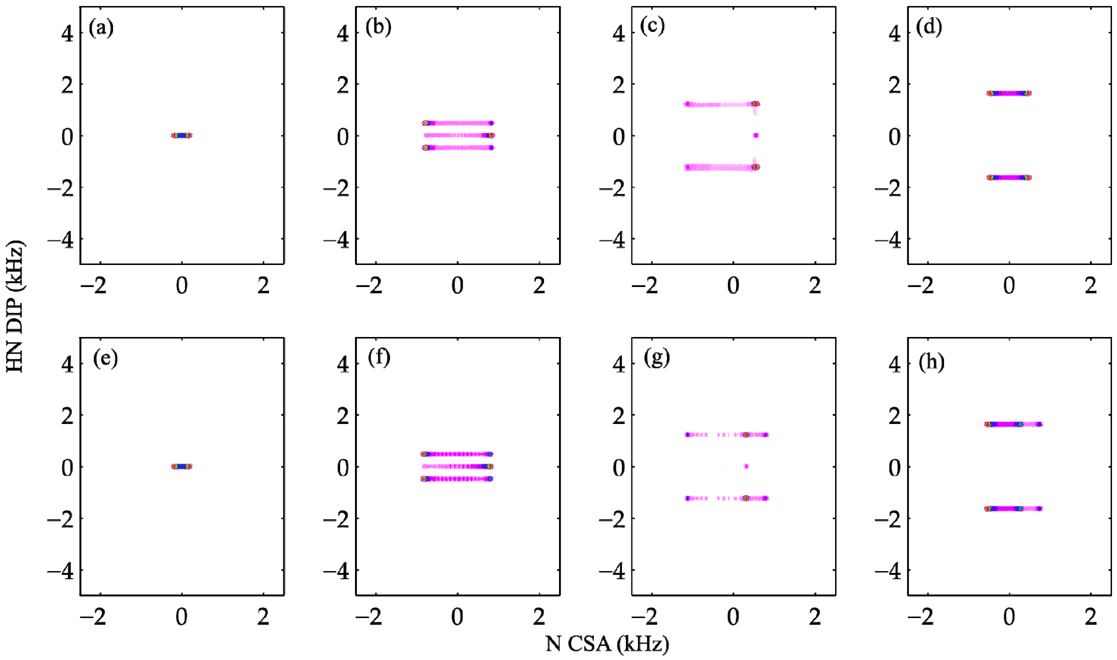

Figure S4. The simulated ^{1}H-^{15}N dipolar and ^{15}N CSA correlation spectra by the combined γ-encoded R18_1^7 / non γ-encoded ROCSA[1] scheme for different crystallite orientations. The same DIP/CSA relative orientation was used for all the simulations. The crystallite orientations expressed in terms of the Euler angles are (a) $\alpha = 0^{\circ}$, $\beta = 0^{\circ}$; (b) $\alpha = 0^{\circ}$, $\beta = 30^{\circ}$; (c) $\alpha = 0^{\circ}$, $\beta = 60^{\circ}$; (d) $\alpha = 0^{\circ}$, $\beta = 90^{\circ}$; (e) $\alpha = 30^{\circ}$, $\beta = 0^{\circ}$; (f) $\alpha = 30^{\circ}$, $\beta = 30^{\circ}$; (g) $\alpha = 30^{\circ}$, $\beta = 60^{\circ}$; (h) $\alpha = 30^{\circ}$, $\beta = 90^{\circ}$. Compared with the R-symmetry based schemes, the non γ-encoded ROCSA sequence results in broad powder pattern along the CSA dimension for each orientation (α, β). The lineshape of the DIP/CSA powder pattern also depends on the relative orientation, but the sensitivity is much lower than in the R-symmetry schemes illustrated in figures S2 and S3. It is therefore necessary to employ γ-encoded recoupling scheme for determination of the CSA tensor orientation in the molecular frame.

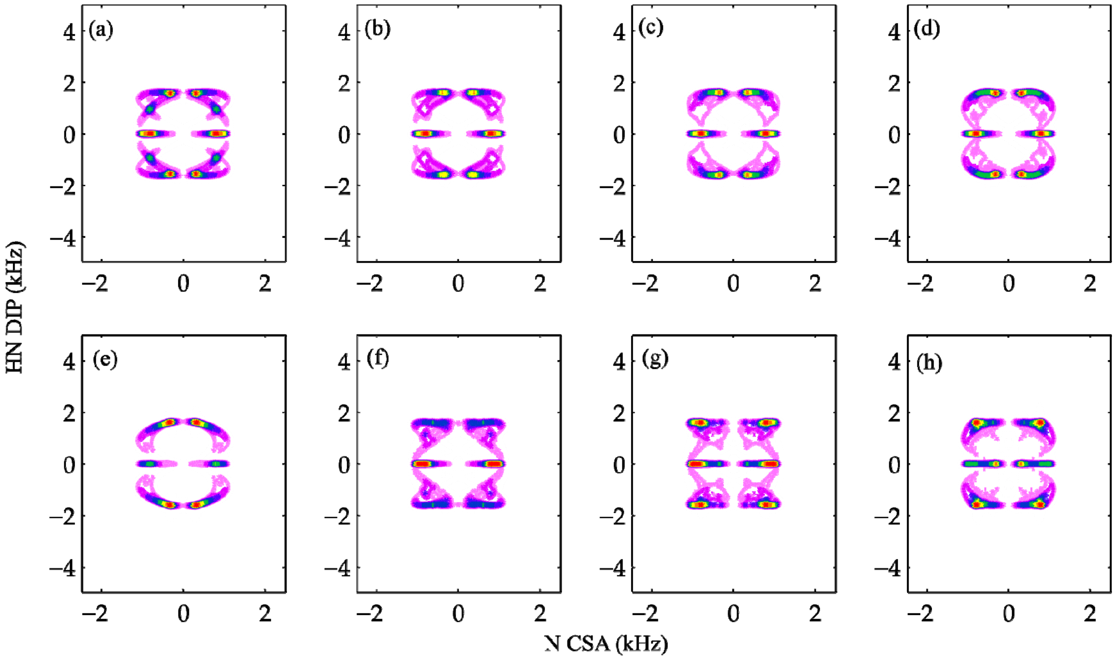

Figure S5. The simulated ^{1}H-^{15}N dipolar and ^{15}N CSA correlation spectra by the combined γ-encoded $R18_1^7/R14_2^5$ scheme for different relative tensor orientations. In a)-d), the Euler angle β_{NH} (the angle between the N-H vector and the CSA δ_{zz} principal value) was 20°, and the Euler angle α_{NH} (the angle between Cα-N-H peptide plane and the CSA δ_{xx} principal value) was 0°, 30°, 60°, and 90°, respectively. In e)-h), the Euler angle α_{NH} was 20°, and β_{NH} was 0°, 30°, 60°, and 90°, respectively. This demonstrates that both Euler angles α_{NH} and β_{NH} affect the 2D correlation spectrum patterns, but the effect of α_{NH} on the lineshape is much less pronounced.

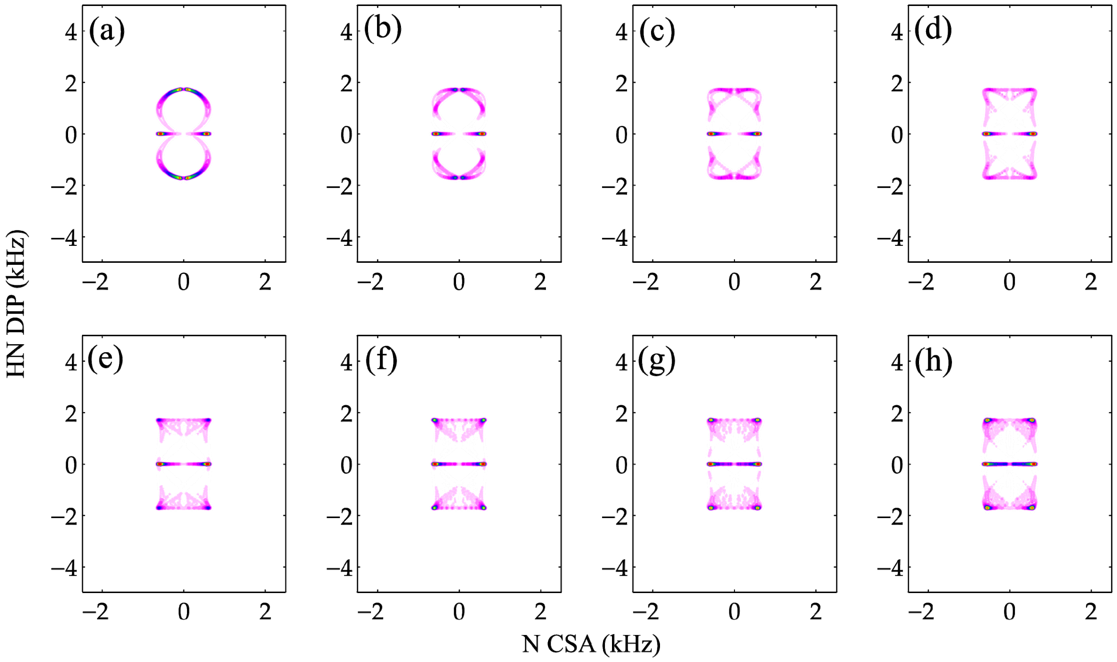

Figure S6. Simulated R18_1^7/R14_2^5 CSA/DIP spectra for different relative tensor orientations. In these simulations, the δ_{xx} principal value CSA is considered to lie in the Cα-N-H peptide plane (α_{NH} = 0°), and the angle β_{NH} between the H-N vector and the CSA δ_{zz} principal value was changed from 0 to 70 degrees with 10-degree increments from (a) to (h), respectively. 64 t_1 increments and 128 t_2 increments were used for each simulation. A powder average was generated with 986 ZCW angles and 3 γ angles.

References:

1. Chan, J. C. C.; Tycko, R., *J. Chem. Phys.,* **2003,** *118*, 8378-8389.